Saudi Pharmaceutical Journal 27 (2019) 968–974

Contents lists available at ScienceDirect

Saudi Pharmaceutical Journal

journal homepage: www.sciencedirect.com

Original article

Antioxidant, antimicrobial and cytotoxic activities of gold nanoparticles capped with quercetin

Felipe Guzansky Milanezi [a], Leandra Martins Meireles [a], Marcella Malavazi de Christo Scherer [a], Jairo P. de Oliveira [b], André Romero da Silva [c], Mariceli Lamas de Araujo [a], Denise Coutinho Endringer [a], Marcio Fronza [a], Marco Cesar Cunegundes Guimarães [b], Rodrigo Scherer [a,*]

[a] Pharmaceutical Sciences Graduate Program, Universidade Vila Velha, 29102-920 Vila Velha, ES, Brazil
[b] Department of Morphology, Federal University of Espírito Santo, 29075-910 Vitória, ES, Brazil
[c] Federal Institute of Espírito Santo, 29192-733 Aracruz, ES, Brazil

ARTICLE INFO

Article history:
Received 17 December 2018
Accepted 10 July 2019
Available online 11 July 2019

Keywords:
Nanotechnology
Flavonoids
Antioxidant
Antimicrobial
Quercetin

ABSTRACT

In the present work, we report the antioxidant, antimicrobial and cytotoxic activities of quercetin-capped gold nanoparticles (AuNPsQct). The synthesis of AuNPsQct was confirmed by UV–Vis spectroscopy, FTIR and transmission electron microscopy (TEM) analyses. The FTIR spectrum showed the integrity of the quercetin molecules on the nanoparticle surface. The TEM images showed sizes less than 100 nm and a slight spherical shape. The electrostatic stability was confirmed by the zeta potential method. The antioxidant activity of quercetin, evaluated by DPPH, ABTS and nitric oxide free radical scavenging methods, was preserved in the gold nanoparticles, furthermore quercetin-capped gold nanoparticles (IR_{50} 0.37 μg/mL) demonstrated a higher antioxidant activity than free quercetin (IR_{50} 0.57 μg/mL) by nitric oxide free radical scavenging method. Strong antifungal activity was observed for *Aspergillus fumigatus* with concentrations ranging from 0.1 to 0.5 mg/mL. The nanoparticles with quercetin did not exhibit cytotoxicity to human fibroblasts (L929 cells). In conclusion, these results suggest that AuNPsQct, produced by cost-effective method, can act as a promising candidate for different medical applications.

1. Introduction

The occurrence of resistant microorganisms, as Aspergillus strains has been reported in several parts of the world to be increasing (Natesan et al., 2013; Pfaller et al., 2011). For the identification of resistant strains, epidemiological cutoff values are established based on minimum inhibitory concentration (MIC) assays to help identify strains with reduced susceptibility (Meletiadis et al., 2012). It is important to emphasize that the occurrence of resistance severely limits treatment options and generates great concern in the medical/scientific community, as well as devastating consequences for the world population. For this reason, studies to find alternatives of natural products with antimicrobial activity are highly encouraging.

Natural antioxidants attract a particular interest because they can protect the human body from free radicals (Amin and Bano, 2018; Houghton, 1995). The production of the reactive oxygen species (ROS), such as nitric oxide (NO), hydroxyl radical (OH) and superoxide anion ($O2^{\cdot-}$) in healthy organisms is balanced by antioxidant defense systems, as well as by the natural antioxidants from vegetables, such as quercetin. However, an organism may be suffering oxidative stress when disturbance in the pro-oxidant–antioxidant balance in favor of the former (Halliwell and Gutteridge, 1990).

Flavonoids are a class of secondary plant phenolics with significant pharmacological activities that have been studied long ago. Among the flavonoids, quercetin (3,5,7,3′-4′-pentahydroxy flavone) is one of the main flavonoids in the human diet and is mainly found in a glycosylated form (quercetin-3-glucoside) in foods. Several studies have indicated pharmacological effects, such as antioxidant activity (Hatahet et al., 2017; Scherer and Godoy, 2009), anti-inflammatory (Hatahet et al., 2017; Lin et al., 2017),

* Corresponding author at: Pharmaceutical Sciences Graduate Program, University of Vila Velha (UVV), Av. Comissário José Dantas de Melo, n°21, 29102-920 Boa Vista, Vila Velha, ES, Brazil.
E-mail address: rodrigo.scherer@uvv.br (R. Scherer).
Peer review under responsibility of King Saud University.

Production and hosting by Elsevier

https://doi.org/10.1016/j.jsps.2019.07.005
1319-0164/

anti-proliferative and anti-angiogenic (de Araújo et al., 2017; Granato et al., 2017), anti-ageing (Chondrogianni et al., 2010), hepatoprotective effect (Miltonprabu et al., 2017), and renoprotective (Guss et al., 2017) effects.

Despite these advantages, a quercetin-free base has a low solubility in water and a low bioavailability and is not well-absorbed orally, limiting its clinical use or use in food formulations (De Souza et al., 2007; Guss et al., 2017; Hatahet et al., 2017; Khor et al., 2017). Thus, nanoscience may be an alternative for solving this low absorption issue since it has presented innumerable innovative solutions, such as the conjugation of antibodies (Jazayeri et al., 2016), vehicles for drug delivery (Chowdhury et al., 2016; Fernandes et al., 2017), UV protection (Ganesan and Gurumallesh Prabu, 2015), antimicrobials (Giteru et al., 2015; Pradeepa et al., 2017), and several others applications.

Among the existing nanomaterials, gold nanoparticles (AuNPs) have attracted attention since gold is an inert material that is resistant to oxidation, which makes its use interesting in nanoscale technologies and devices (Bindhu and Umadevi, 2014). In addition, AuNPs are well understood with regard to their reduction and functionalization with synthetic and natural products. On the other hand, the pharmacological properties must be preserved after the capping process, that is, the synthesis process cannot reduce the biological properties of the bioactive compound, and furthermore, exhibit low toxicity. Thus, nanotechnology can be a promising method to create new formulations with the aim of improving the biological activity of quercetin and potentiating the activity of this molecule. Therefore, the aim of this work was to synthesize and characterize gold nanoparticles capped with quercetin (AuNPsQct) and to evaluate its antioxidant, antimicrobial and cytotoxic activities in comparison with free quercetin.

2. Material and methods

2.1. Synthesis and characterization of gold nanoparticles with quercetin

Gold nanoparticles (AuNPs) were synthesized according Pal et al. (2013) with slight modifications. Briefly, 15 mL of a $HAuCl_4$ solution (0.1 g/L, pH 5.0) was used and maintained under stirring at 600 rpm at 90 °C. Then, 1 mL of an aqueous sodium citrate solution (10 g/L) was added with stirring for 10 min. The red colour confirmed the formation of the AuNPs. After, ethanolic solutions of quercetin were added with an additional 5 min of shaking. This procedure was performed at concentrations of 0.17 mg/mL, 0.85 mg/mL, 1.7 mg/mL and 8.5 mg/mL of quercetin.

2.2. Characterization by UV–Visible spectroscopy

The absorbance readings of the nanoparticle samples were performed using an Evolution® 300 Thermo Scientific Spectrophotometer. The readings were taken at 250–700 nm with a scanning speed of 600 nm/min.

2.3. Characterization by FTIR analysis

Infrared analysis was performed in the ATR mode on an FTIR/FTNIR Spectrum 400, PerkinElmer using potassium bromide (KBr) for dehydration after centrifugation of the material at 8608*g* for 10 min. All bands were analysed in the absorption bands from 650 to 4000 cm^{-1} by Origin Pro 8.5 software (Trial Version).

2.4. Characterization by transmission electron microscopy (TEM)

The AuNPsQct were examined in a Transmission Electron Microscope (JEM-1400, JEOL, USA), with a lanthanum hexaboride (LaB_6) filament operated at 120 kV. Approximately 5 μL of each sample solution were placed onto copper (400 mesh) grids containing a Formvar resin support film (polyvinyl formal resin) and dried at room temperature. TEM images were taken to verify the size and shape distribution of the synthesized AuNPsQct.

2.5. Evaluation of the stability by the zeta potential method

Approximately 2 mL of each sample solution were analysed in a Microtrac Zetatrac particle analyser, and the values were related to the mean of the readings and were expressed in mV.

2.6. Freeze-drying of the nanoparticles

The nanoparticles were frozen at −80 °C (Ultra-freezer CL580, Cold Lab) and freeze dried (Enterprise I, Terroni, Brazil) for 24 h or until the formation of a completely dehydrated powder of reddish colour.

2.7. Entrapment efficiency

The determination of the quercetin entrapment efficiency was performed by the Folin–Ciocalteau method, as previously described by Scherer and Godoy (2014), adapted for 96-well microplates. A 30 μL aliquot of the AuNPsQct (0.5 mg/mL) and 150 μL of the Folin reagent, diluted in distilled water (1/10), were added into each well. After 5 min, 120 μL of a 7.5% aqueous solution of sodium carbonate was added to the system. The reaction occurred for 1 h in darkness, and the absorbance was monitored at 740 nm. All analyses were done in hexaplicate. The results were expressed as quercetina by an external calibration curve with free quercetin.

2.8. Antioxidant activity

2.8.1. DPPH free radical scavenging

The antioxidant activity of quercetin and AuNPsQct was determined by the free radical scavenging method according to Scherer and Godoy (2009), which was adapted for 96-well microplates. An aliquot of 280 μL of DPPH (40 μg/mL; ethanol solution) and 20 μL of the quercetin or AuNPsQct solutions at concentrations of 100 μg/mL to 2 μg/mL (serial dilution) were used, and a blank 20 μL of ethanol was used. All tests were performed in triplicate. The microplates were kept in the dark at room temperature for 90 min, and after that period the absorbance was measured at 517 nm using a microplate reader (Molecular Devices, Spectra Max 190, USA). The scavenging activity of the radicals was calculated according to the equation: $I\% = [(Abs0 - Abs1)/Abs0] \times 100$, where Abs0 is the absorbance of the blank and Abs1 is the absorbance of the test. IR_{50} (sufficient amount for 50% reduction) was calculated by the equation of the calibration curve (5 points).

2.8.2. ABTS free radical scavenging

The antioxidant activity was determined by the ABTS free radical scavenging method, according to Re et al. (1999)), modified by Guss et al. (2017). Initially, the radical $ABTS^{+}$ was formed by mixing 7.0 mM ABTS (50% ethanol) containing 2.45 mM potassium persulphate (distilled water). This reagent was stored under refrigeration for at least 16 h. Before use, the reagent was diluted with 50% ethanol until an absorption of 1.0 (±0.01) at 734 nm. $ABTS^{+}$ (270 μL) and 30 μL of each concentration (100–2 μg/mL) of the compounds were added to the 96-well microplates. Ethanol (30 μL) was added to the blank. After 10 min of the reaction in the dark, a reading was

taken at 734 nm using the microplate reader (Molecular Devices, Spectra Max 190, USA). The radical scavenging activity was calculated as follows: I% = [(Abs0 − Abs1)/Abs0] × 100, where Abs0 is the blank absorbance and ABS1 is the test absorbance. The results were expressed as IR_{50} (concentration reducing 50% of free radicals), which was calculated by the calibration curve.

2.8.3. Nitric oxide free radical scavenging

The determination of NO sequestration was evaluated using sodium nitroprusside (NPS) as a nitrite donor according to the methodologies of Green et al. (1982) and Maia et al. (2010) with modifications. In a 96-well plate, 75 μL of the samples (7.8–1000 μg/mL) and 75 μL of NPS (1.25 mM) were added and incubated for 5 min in ultraviolet light. Then, 75 μL of 1% sulphanilamide and 75 μL of 0.1% N-1-naphthalylethylenediamine dihydrochloride were added. As a positive control, gallic acid (14 μg/mL) was used. The concentration of nitrite generated from the spontaneous decomposition of NPS was calculated by linear regression using a standard solution of sodium nitrite in a microplate reader (Elisa Spectra count, Packard - USA) at 540 nm.

2.9. Antimicrobial activity

For the evaluation of the antibacterial activity, the species of *Escherichia coli* (ATCC 8739), *Staphylococcus aureus* (ATCC 25923), *Salmonella typhimurium* (ATCC 14028) and *Bacillus cereus* (ATCC 14579) were obtained from the list of reference strains of INCQS-FIOCRUZ. The MIC determination was performed by a microdilution method, according to the Clinical and Laboratory Standards Institute (CLSI) reference protocol M26-A (CLSI, 1999). The final concentration of the cells was adjusted with Mueller-Hinton broth in a spectrophotometer at 625 nm with an optical density of 0.08–0.1 to obtain a concentration of 5×10^5 CFU/mL. The assay was performed in the 96-well plates by the addition of 150 μL of the inoculum and 150 μL of the sample to final concentrations of 2.0 mg/mL and 0.016 mg/mL, respectively. The positive control wells (Mueller-Hinton broth with DMSO and inoculum) and negative control (Mueller-Hinton Broth with DMSO) were inserted in all plates, and all analyses were performed in triplicate. The plates were incubated at 36 °C for 24 h, and then 50 μL of the CTT (0.5% in aqueous solution) was added. After 6 h of incubation, the minimum inhibitory concentration (MIC) was determined to be the lowest concentration capable of inhibiting the visible growth of cells conferred by CTT (the dead cells were not stained).

For the antifungal activity, three clinical isolates of *Aspergillus fumigatus* [AF 293(PyrG+), WT 35, and CEA17(PyrG+)], donated by the University of Sao Paulo (USP) of Ribeirão Preto, were used. The MIC determination was performed by the microdilution method, according to the CLSI reference protocol M38-A2 (CLSI, 2008). The isolated fungi were grown on potato dextrose agar for 7 days at 36 °C to induce spore formation, after which they were collected with sterile saline (0.85%) and Tween 20 (0.05%). The final concentration of the cells was adjusted in a spectrophotometer at 530 nm with an optical density ranging from 0.09 to 0.13 to obtain a concentration of 5×10^4 CFU/mL. The concentrations of the sample range between 2.0 mg/mL and 0.016 mg/mL. The positive control wells (RPMI broth with DMSO and inoculum) and negative control (RPMI broth with DMSO) were inserted in all plates, and all analyses were performed in triplicate. The 96-well microplates were incubated at 36 °C, and the results were analysed after 48 h. The results were given by identifying the MIC, which was visually identified with the aid of a reading mirror.

2.10. Cytotoxic activity

The *in vitro* cytotoxic activity was evaluated in the colorimetric MTT assay (Mosmann, 1983). An aliquot of 150 μL of the L929 fibroblasts cells at a concentration of 7×10^5 cells/mL was added into the 96-well microplate and incubated for 24 h at 37 °C in an atmosphere of 5% CO_2. After 24 h, the cells were treated with increasing concentrations of the AuNPs, AuNPsQct, and quercetin (0.2–25.0 μg/mL), and the plates were incubated for 24 h. After incubation, the contents of the wells were removed, and then 100 μL of MTT (5 mg/mL) was added to each well and incubated for an additional 2 h to allow the reaction of MTT by cellular mitochondrial dehydrogenases. Then, the medium was removed, and 100 μL of DMSO were added to dissolve the formazan crystals. The absorbance of purple formazan, proportional to the number of viable cells, was measured at 595 nm using the microplate reader (Molecular Devices, Spectra Max 190, USA). The results are expressed as a percentage and as IC_{50} (a concentration that kills 50% of the cells).

2.11. Statistical analysis

The statistical analysis was performed by a one-way analysis of variance (ANOVA) using BioEstat 5.0 software. When the ANOVA showed significant differences, the Tukey's test was used for post hoc analysis ($p < 0.05$).

3. Results

3.1. Characterization by UV–Visible spectroscopy and the entrapment efficiency

Gold nanoparticles were synthesized by the reduction of AuCl4 using sodium citrate as the reducing agent. The characteristic localized surface plasmon resonance (LSPR) band was observed at 520 nm, and the colour change of the sample ranged from red to violet shades, which indicated the successful synthesis of AuNPs (Fig. 1).

In addition, we noticed that the lower concentration of the nanoparticles had the highest signal intensity (Fig. 1). A bathochromic shift can also be verified by the presence of quercetin in gold nanoparticles. In this way, the subsequent tests were performed with a concentration of 0.17 mg/mL. After freeze drying, a reddish-coloured powder was obtained and was used to evaluate

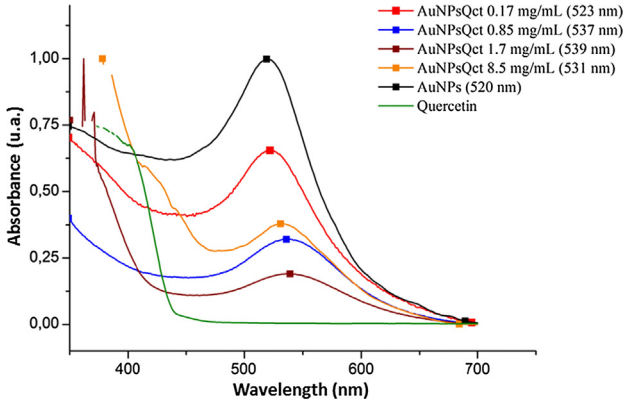

Fig. 1. UV–Visible absorption spectra of gold nanoparticles with quercetin (AuNPsQct), gold nanoparticles without quercetin (AuNPs), and free quercetin; (maximum wavelength).

the entrapment efficiency, and the result was 79%, which is very similar to a previous study that reported 77% (Pal et al., 2013).

3.2. Characterization by FTIR

FTIR analysis confirmed quercetin capping on the AuNPs (AuNPsQct) by showing the signature peaks of quercetin at 3248 cm^{-1} (O—H stretching), 1670 cm^{-1} (C=O stretching) and 1500 cm^{-1} (C=C stretching). Moreover, the absorption bands in the region between 650 and 1000 cm^{-1} related to the angular deformation of C=CH of the aromatic compounds were observed, which corroborates with a previous study (Pal et al., 2013) (Fig. 2).

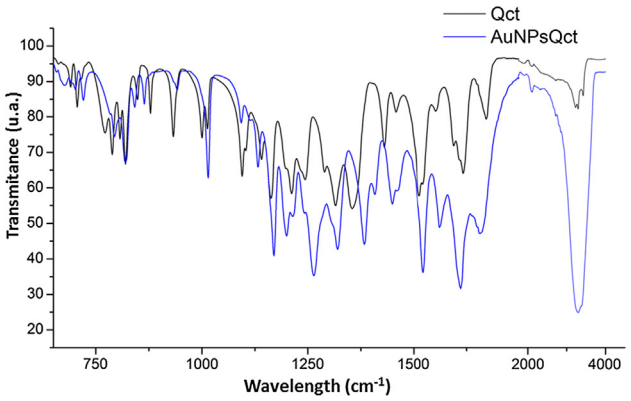

Fig. 2. Characterization by FTIR of free quercetin (Qct) and gold nanoparticles with quercetin (AuNPsQct) at 0.17 mg/mL.

3.3. Characterization by transmission electron microscopy (TEM) and a zeta potential method

TEM images revealed that the AuNPsQct are structurally quasi-spherical and presented sizes smaller than 100 nm, and particles are relatively monodisperse under these nucleation and growth conditions (Fig. 3). Analyses of the colloidal stability were performed by zeta potential measurements. The AuNps with 0.17 mg/mL quercetin show the best stability (−54,80 mv). Moreover, the AuNPsQct shifted to a negative charge due the high amount of hydroxyl radical charges (Fig. 4).

3.4. Antioxidant activity

The antioxidant activity was determined by the DPPH, ABTS and nitric oxide free radical scavenging methods, and it was observed that both free quercetin and AuNPsQct showed antioxidant activity in all methods, demonstrating that the antioxidant capacity of quercetin was preserved in the nanoparticles (Table 1). No significant difference in the DPPH method was observed. In the ABTS assay, free quercetin presented a lower IR_{50} than AuNPsQct. On the other hand, in the nitric oxide scavenging assay, the reverse was observed, where the AuNPsQct IR_{50} was significantly lower ($p < 0.05$).

3.5. Antimicrobial activity

Quercetin and AuNPsQct showed excellent antifungal activity against *A. fumigatus* strains isolated from patients with aspergillosis (Table 2). This result makes AuNPsQct a promising drug for the treatment of aspergillosis since gold nanoparticles are already used

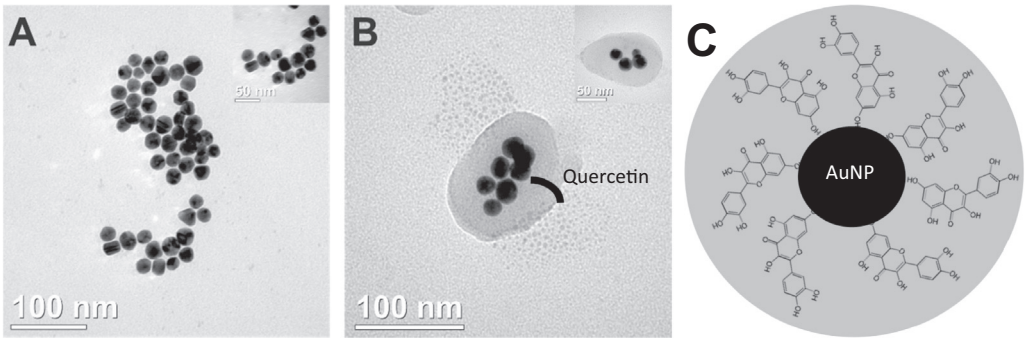

Fig. 3. Ultrastructure of the gold nanoparticles and gold nanoparticles with quercetin by transmission electron microscopy. (A) AuNPs, (B) AuNPsQct and (C) illustration.

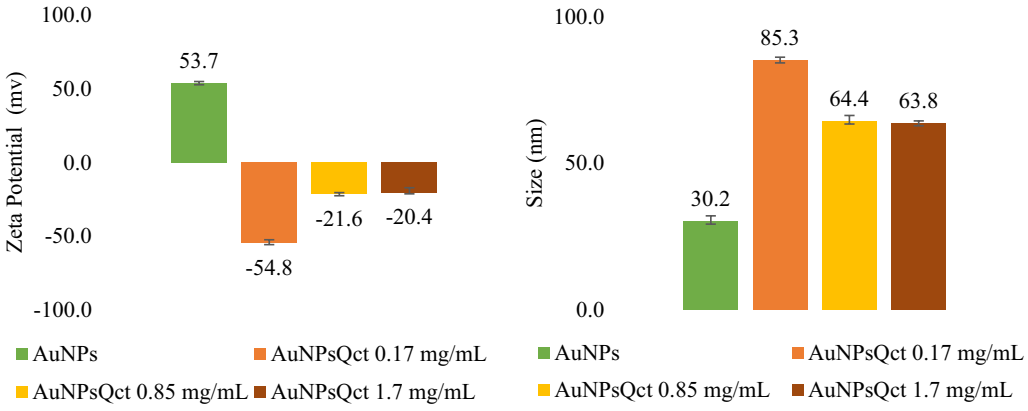

Fig. 4. Zeta potential (ZP) and mean size of gold nanoparticles with quercetin (AuNPsQct), gold nanoparticles without quercetin (AuNPs).

Table 1
Antioxidant activity of the quercetin and gold nanoparticle samples.

Samples	DPPH IR_{50} (μg/mL)	ABTS IR_{50} (μg/mL)	Nitric oxide IR_{50} (μg/mL)
Quercetin	2.04 ± 0.04 a	3.05 ± 0.27 a	0.57 ± 0.06 b
AuNPsQct	2.09 ± 0.09 a	4.22 ± 0.54 b	0.37 ± 0.01 a

Different letters in the same column correspond to the significant difference ($p < 0.05$). AuNPsQct: gold nanoparticles with quercetin.

Table 2
Minimum inhibitory concentration of the quercetin and gold nanoparticle samples.

Microorganism	Quercetin mg/mL	AuNPsQct mg/mL	AuNPs mg/mL
S. aureus	2.0	2.0	–
B. cereus		–	–
E. coli	–	–	–
S. typhimurium	–	–	–
A. fumigatus WT35	0.2	0.38	–
A. fumigatus AF293	0.1	0.15	–
A. fumigatus CEA17	0.2	0.15	–

AuNPsQct: gold nanoparticles with quercetin, AuNPs: gold nanoparticles without quercetin, –: no activity.

for drug delivery. On the other hand, the results against bacteria revealed that the nanoparticles did not alter the activity of quercetin, presenting activity only against *S. aureus* at a concentration of 2.0 mg/mL.

3.6. Cytotoxic activity

Both AuNPsQct and free quercetin showed no cytotoxicity for the L929 fibroblast cells, since no significant differences were observed between the control (Fig. 5). Previous study reported no cytotoxic activity of gold nanoparticles capped with quercetin (June et al., 2016),

4. Discussion

The UV–Vis scanning spectrum showed that AuNPsQct demonstrate absorption bands between 500 and 600 nm, which can be attributed to localized surface plasmon resonance (LSPR). This is an optical property of noble metals, such as gold, which manifests in the visible region (400–700 nm) of the electromagnetic spectrum (Petryayeva and Krull, 2011; Shameli et al., 2012).

The infrared spectra recorded similar characteristics, albeit with a lower intensity of the quercetin molecules present after the synthesis of the AuNPs, which occurred through irreversible electrostatic interactions. The presence of all other characteristic bands

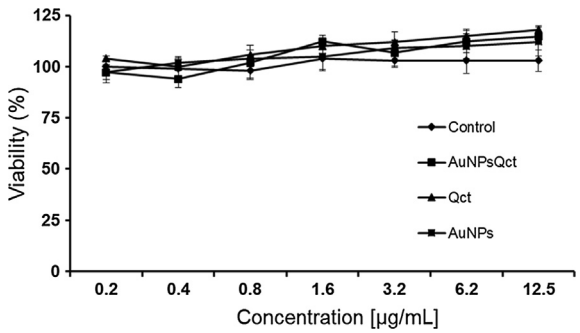

Fig. 5. Evaluation of the cell viability by the MTT colorimetric method of gold nanoparticles with quercetin (AuNPsQct), gold nanoparticles without quercetin (AuNPs), and free quercetin (Qct).

of quercetin in the IR spectrum of AuNPsQct indicated that the structure of quercetina remained unaltered in the complex, corroborating with a previous study (Pal et al., 2013). In addition, it was observed that both quercetin and AuNPsQct presented strong antioxidant activity, thus guaranteeing that the nanoparticles preserve this recognized property of quercetin. This fact is important for therapeutic applications of AuNPsQct and can be explained by the fact that phenolic hydroxyls (Fig. 3C), responsible for antioxidant activity, do not participate in binding with citrate, as reported by previous work (Pal et al., 2013). Moreover, in the nitric oxide method, the AuNPsQct presented higher antioxidant activity than free quercetin, a remarkable fact for future use of the synthesized material.

Regarding the stability of the AuNPs, their relationship is directly proportional to the zeta potential (ZP), which reflects the surface potential of the particles, which is influenced by the changes in the interface with the dispersing medium, due to the dissociation of the functional groups in the surface of the particle or the adsorption of the ionic species present in the aqueous medium. It was observed that the AuNPsQct presented a negative ZP, and the AuNPs showed a positive ZP. This change in electric charge confirms the colloidal stability through the zeta potential method. The value of the ZP indicated that the levelling molecules present on the surface of AuNPsQct are composed mainly of negatively charged groups. These groups are responsible for the stability of AuNPsQct since quercetin is a strong reducing agent, which may aid in the stabilization of AuNPs. The carboxylate group present on the outer surface of the AuNPs can also act as a surfactant to fix to the surface of the same and stabilize it through electrostatic stabilization, which is a fundamental property mainly pharmacological and biomedical applications (Bhattacharjee, 2016; Lee et al., 2015).

The results showed that the antibacterial and antifungal activities of AuNPsQct and quercetin were similar. Despite this, an advantage in the use of AuNPsQct is the possible penetration into the cellular membranes, which increases the antibacterial effect and the direction of the drug, favouring its biological activity (Uma Suganya et al., 2015). The antifungal action of AuNPsQct against *A. fumigatus* shows MIC values that the literature points to as promising values for new molecules (Cos et al., 2006); however, the mechanism of action is still not well elucidated. On possible mechanism is that AuNPsQct generated fungal wall dysfunction, resulting in the loss of intracellular ions and liquids or the inactivation of key enzymes, which consequently lead to cell death (L. and M., 2017). Clinically, this result is interesting since *A. fumigatus* is one of the major causes of aspergillosis since they are found abundantly in air (80–90%) and are generally harmless. However, in patients with a weakened immune system, *A. fumigatus* can be a great cause of diseases leading to death. The weak activity against bacteria may be due to the complexity of the external membrane with a layer of peptidoglycan and the other three components that surround the cell wall (Guo et al., 2016). Finally, we emphasize that no cytotoxicity activity was observed in any tested concentration of quercetin nanoparticles, agreeing with a previous study, which reports no cytotoxicity activity for quercetin-gadolinium complex (Muthurajan et al., 2015).

5. Conclusion

The synthesized AuNPsQct with a 79% entrapment efficiency demonstrated spherical shapes and an average size less than 100 nm, and the colloidal stability was confirmed by the zeta potential method. The characterization analyses clearly confirm that there was no change in the molecular structure of quercetin, and the phenolic hydroxyls responsible for the main

pharmacological activities, as an antioxidant, were preserved. This hypothesis was confirmed by the antioxidant assays, where the results showed strong activity. Additionally, by the nitric oxide free radical scavenging method, the activity for AuNPsQct was significantly higher than that of free quercetin. No cytotoxic effects were observed on the L929 fibroblast cells for both free quercetin and AuNPsQct in the tested concentrations. A potent antifungal action against the strains of *A. fumigatus* isolated from patients with aspergillosis was verified.

Acknowledgements

The Fundação de Amparo à Pesquisa do Espírito Santo (FAPES) and the Coordenação de Aperfeiçoamento de Pessoal de Nível Superior (CAPES) are greatly acknowledged for the financial support.

Declaration of conflict of interest

The authors declare no conflict of interest.

References

Amin, F., Bano, B., 2018. Damage of cystatin due to ROS-generation and radical-scavenging activity of antioxidants and associated compounds. Int. J. Biol. Macromol. 119, 369–379. https://doi.org/10.1016/j.ijbiomac.2018.07.100.

Bhattacharjee, S., 2016. DLS and zeta potential - What they are and what they are not? J. Control. Release 235, 337–351. https://doi.org/10.1016/j.jconrel.2016.06.017.

Bindhu, M.R., Umadevi, M., 2014. Antibacterial activities of green synthesized gold nanoparticles. Mater. Lett. 120, 122–125. https://doi.org/10.1016/j.matlet.2014.01.108.

Chondrogianni, N., Kapeta, S., Chinou, I., Vassilatou, K., Papassideri, I., Gonos, E.S., 2010. Anti-ageing and rejuvenating effects of quercetin. Exp. Gerontol. 45, 763–771. https://doi.org/10.1016/j.exger.2010.07.001.

Chowdhury, S., Yusof, F., Salim, W.W.A.W., Sulaiman, N., Faruck, M.O., 2016. An overview of drug delivery vehicles for cancer treatment: nanocarriers and nanoparticles including photovoltaic nanoparticles. J. Photochem. Photobiol. B Biol. 164, 151–159. https://doi.org/10.1016/j.jphotobiol.2016.09.013.

CLSI, 2008. Reference Method for Broth Dilution Antifungal Susceptibility Testing of Filamentous Fungi; Approved Standard — Second Edition. CLSI document M38-A2. Clinical and Laboratory Standards Institute, Clinical and Laboratory Standards Institute, Wayne, PA.

CLSI, 1999. Methods for Determining Bactericidal Activity of Antimicrobial Agents; Approved Guideline. CLSI document M26-A. Clinical and Laboratory Standards Institute, Wayne, PA. Clin. Lab. Stand. Inst. 19.

Cos, P., Vlietinck, A.J., Berghe, D. Vanden, Maes, L., 2006. Anti-infective potential of natural products: how to develop a stronger in vitro "proof-of-concept". J. Ethnopharmacol. 106, 290–302. https://doi.org/10.1016/j.jep.2006.04.003.

de Araújo, R.F., de Araújo, A.A., Pessoa, J.B., Freire Neto, F.P., da Silva, G.R., Leitão Oliveira, A.L.C.S., de Carvalho, T.G., Silva, H.F.O., Eugênio, M., Sant'Anna, C., Gasparotto, L.H.S., 2017. Anti-inflammatory, analgesic and anti-tumor properties of gold nanoparticles. Pharmacol. Rep. 69, 119–129. https://doi.org/10.1016/j.pharep.2016.09.017.

De Souza, K.C.B., Bassani, V.L., Schapoval, E.E.S., 2007. Influence of excipients and technological process on anti-inflammatory activity of quercetin and Achyrocline satureioides (Lam.) D.C. extracts by oral route. Phytomedicine 14, 102–108. https://doi.org/10.1016/j.phymed.2005.10.007.

Fernandes, A.R., Jesus, J., Martins, P., Figueiredo, S., Rosa, D., Martins, L.M.R.D.R.S., Corvo, M.L., Carvalheiro, M.C., Costa, P.M., Baptista, P.V., 2017. Multifunctional gold-nanoparticles: a nanovectorization tool for the targeted delivery of novel chemotherapeutic agents. J. Control. Release 245, 52–61. https://doi.org/10.1016/j.jconrel.2016.11.021.

Ganesan, R.M., Gurumallesh Prabu, H., 2015. Synthesis of gold nanoparticles using herbal Acorus calamus rhizome extract and coating on cotton fabric for antibacterial and UV blocking applications. Arab. J. Chem. https://doi.org/10.1016/j.arabjc.2014.12.017. in press.

Giteru, S.G., Coorey, R., Bertolatti, D., Watkin, E., Johnson, S., Fang, Z., 2015. Physicochemical and antimicrobial properties of citral and quercetin incorporated kafirin-based bioactive films. Food Chem. 168, 341–347. https://doi.org/10.1016/j.foodchem.2014.07.077.

Granato, M., Rizzello, C., Montani, M.S.G., Cuomo, L., Vitillo, M., Santarelli, R., Gonnella, R., D'Orazi, G., Faggioni, A., Cirone, M., 2017. Quercetin induces apoptosis and autophagy in primary effusion lymphoma cells by inhibiting PI3K/AKT/mTOR and STAT3 signaling pathways. J. Nutr. Biochem. 41, 124–136. https://doi.org/10.1016/j.jnutbio.2016.12.011.

Green, L.C., Wagner, D.A., Glogowski, J., Skipper, P.L., Wishnok, J.S., Tannenbaum, S. R., 1982. Analysis of nitrate, nitrite, and [15N]nitrate in biological fluids. Anal. Biochem. 126, 131–138. https://doi.org/10.1016/0003-2697(82)90118-X.

Guo, Y., Wang, Yu., Liu, S., Yu, J., Wang, H., Wang, Yalin, Huang, J., 2016. Label-free and highly sensitive electrochemical detection of E. coli based on rolling circle amplifications coupled peroxidase-mimicking DNAzyme amplification. Biosens. Bioelectron. 75, 315–319. https://doi.org/10.1016/j.bios.2015.08.031.

Guss, K.L., Pavanni, S., Prati, B., Dazzi, L., de Oliveira, J.P., Nogueira, B.V., Pereira, T.M. C., Fronza, M., Endringer, D.C., Scherer, R., 2017. Ultrasound-assisted extraction of Achyrocline satureioides prevents contrast-induced nephropathy in mice. Ultrason. Sonochem. 37, 368–374. https://doi.org/10.1016/j.ultsonch.2017.01.035.

Halliwell, B., Gutteridge, J.M.C., 1990. The antioxidants of human extracellular fluids. Arch. Biochem. Biophys. 280, 1–8. https://doi.org/10.1016/0003-9861(90)90510-6.

Hatahet, T., Morille, M., Shamseddin, A., Aubert-Pouëssel, A., Devoisselle, J.M., Bégu, S., 2017. Dermal quercetin lipid nanocapsules: Influence of the formulation on antioxidant activity and cellular protection against hydrogen peroxide. Int. J. Pharm. 518, 167–176. https://doi.org/10.1016/j.ijpharm.2016.12.043.

Houghton, P.J., 1995. The role of plants in traditional medicine and current therapy. J. Altern. Complement. Med. 1, 131–143. https://doi.org/10.1089/acm.1995.1.131.

Jazayeri, M.H., Amani, H., Pourfatollah, A.A., Pazoki-Toroudi, H., Sedighimoghaddam, B., 2016. Various methods of gold nanoparticles (GNPs) conjugation to antibodies. Sens. Bio-Sensing Res. 9, 17–22. https://doi.org/10.1016/j.sbsr.2016.04.002.

June, P., Eun, P., Go, B., Hee, M., Dong, H., Lee, G., Ju, M., 2016. Evaluation of the cytotoxicity of gold nanoparticle-quercetin complex and its potential as a drug delivery vesicle. J. Appl. Biol. Chem. 59, 145–147.

Khor, C.M., Ng, W.K., Kanaujia, P., Chan, K.P., Dong, Y., 2017. Hot-melt extrusion microencapsulation of quercetin for taste-masking. J. Microencapsul. 34, 29–37. https://doi.org/10.1080/02652048.2017.1280095.

L., Y., M., S., 2017. Myelodysplastic syndrome with aspergillus fumigatus infection: a case report and literature review. Radiol. Infect. Dis. 4, 26–28. https://doi.org/10.1016/j.jrid.2016.07.008.

Lee, K.D., Nagajyothi, P.C., Sreekanth, T.V.M., Park, S., 2015. Eco-friendly synthesis of gold nanoparticles (AuNPs) using Inonotus obliquus and their antibacterial, antioxidant and cytotoxic activities. J. Ind. Eng. Chem. 26, 67–72. https://doi.org/10.1016/j.jiec.2014.11.016.

Lin, X., Lin, C.H., Zhao, T., Zuo, D., Ye, Z., Liu, L., Lin, M.T., 2017. Quercetin protects against heat stroke-induced myocardial injury in male rats: Antioxidative and antiinflammatory mechanisms. Chem. Biol. Interact. 265, 47–54. https://doi.org/10.1016/j.cbi.2017.01.006.

Maia, R.M., Moura, C.W.N., Bispo, V.S., Santos, J.L.A., Santana, R.S., Matos, H.R., 2010. Avaliação do sequestro do óxido nítrico (NO) pelo extrato metanólico da alga Bryothamnion triquetrum (Gmelin) Howe. Brazilian J. Pharmacogn. 20, 489–493. https://doi.org/10.1590/S0102-695X2010000400005.

Meletiadis, J., Mavridou, E., Melchers, W.J.G., Mouton, J.W., Verweij, P.E., 2012. Epidemiological cutoff values for azoles and Aspergillus fumigatus based on a novel mathematical approach incorporating cyp51A sequence analysis. Antimicrob. Agents Chemother. 56, 2524–2529. https://doi.org/10.1128/AAC.05959-11.

Miltonprabu, S., Tomczyk, M., Skalicka-Woźniak, K., Rastrelli, L., Daglia, M., Nabavi, S.F., Alavian, S.M., Nabavi, S.M., 2017. Hepatoprotective effect of quercetin: from chemistry to medicine. Food Chem. Toxicol. 108, 365–374. https://doi.org/10.1016/j.fct.2016.08.034.

Mosmann, T., 1983. Rapid colorimetric assay for cellular growth and survival: application to proliferation and cytotoxicity assays 65, 55–63.

Muthurajan, T., Rammanohar, P., Rajendran, N.P., Sethuraman, S., Krishnan, U.M., 2015. Evaluation of a quercetin-gadolinium complex as an efficient positive contrast enhancer for magnetic resonance imaging. RSC Adv. 5, 86967–86979. https://doi.org/10.1039/c5ra16405b.

Natesan, S.K., Lamichchane, A.K., Swaminathan, S., Wu, W., 2013. Differential expression of ATP-binding cassette and/or major facilitator superfamily class efflux pumps contributes to voriconazole resistance in Aspergillus flavus. Diagn. Microbiol. Infect. Dis. 76, 458–463. https://doi.org/10.1016/j.diagmicrobio.2013.04.022.

Pal, R., Panigrahi, S., Bhattacharyya, D., Chakraborti, A.S., 2013. Characterization of citrate capped gold nanoparticle-quercetin complex: Experimental and quantum chemical approach. J. Mol. Struct. 1046, 153–163. https://doi.org/10.1016/j.molstruc.2013.04.043.

Petryayeva, E., Krull, U.J., 2011. Localized surface plasmon resonance: nanostructures, bioassays and biosensing-A review. Anal. Chim. Acta 706, 8–24. https://doi.org/10.1016/j.aca.2011.08.020.

Pfaller, M., Boyken, L., Hollis, R., Kroeger, J., Messer, S., Tendolkar, S., Diekema, D., 2011. Use of epidemiological cutoff values to examine 9-year trends in susceptibility of Candida species to anidulafungin, caspofungin, and micafungin. J. Clin. Microbiol. 49, 624–629. https://doi.org/10.1128/JCM.02120-10.

Pradeepa, Udaya-Bhat, K., Vidya, S.M., 2017. Nisin gold nanoparticles assemble as potent antimicrobial agent against Enterococcus faecalis and Staphylococcus aureus clinical isolates. J. Drug Deliv. Sci. Technol. 37, 20–27. https://doi.org/10.1016/j.jddst.2016.11.002.

Re, Roberta, Pelegrini, Nicoletta, Proteggente, Anna, Pannala, Ananth, M.Y., C.R.-E., 1999. Antioxidant activity applying an improved abts radical. Free Radic. Biol. Med. 26, 1231–1237.

Scherer, R., Godoy, H., 2014. Effects of extraction methods of phenolic compounds from Xanthium strumarium L. and their antioxidant activity. Rev. Bras. Plantas Med. 16, 41–46. https://doi.org/10.1590/S1516-05722014000100006.

Scherer, R., Godoy, H.T., 2009. Antioxidant activity index (AAI) by the 2,2-diphenyl-1-picrylhydrazyl method. Food Chem. 112, 654–658. https://doi.org/10.1016/j.foodchem.2008.06.026.

Shameli, K., Ahmad, M. Bin, Jaffar Al-Mulla, E.A., Ibrahim, N.A., Shabanzadeh, P., Rustaiyan, A., Abdollahi, Y., Bagheri, S., Abdolmohammadi, S., Usman, M.S., Zidan, M., 2012. Green biosynthesis of silver nanoparticles using callicarpa maingayi stem bark extraction. Molecules 17, 8506–8517. https://doi.org/10.3390/molecules17078506.

Uma Suganya, K.S., Govindaraju, K., Ganesh Kumar, V., Stalin Dhas, T., Karthick, V., Singaravelu, G., Elanchezhiyan, M., 2015. Blue green alga mediated synthesis of gold nanoparticles and its antibacterial efficacy against Gram positive organisms. Mater. Sci. Eng. C 47, 351–356. https://doi.org/10.1016/j.msec.2014.11.043.